

Silver(I) bromide complexes of the rigid diphosphanes  
1,2-bis(diphenylphosphano)benzene (dppbz)  
and 4,5-bis(diphenylphosphano)-9,9-dimethyl-xanthene (xantphos):  
Crystal structures of  $[\text{Ag}(\mu_2\text{-Br})(\text{dppbz})]_2$ ,  $[\text{AgBr}(\text{xantphos})]$   
and  $[\text{AgBr}(\text{xantphos})(\text{py2SH})]$

A. Kaltzoglou<sup>a</sup>, P.J. Cox<sup>b</sup>, P. Aslanidis<sup>c,\*</sup>

<sup>a</sup> Department Chemie, Technische Universität München, Lichtenbergstr., 4, D-85747 Garching, Germany

<sup>b</sup> School of Pharmacy, The Robert Gordon University, Schoolhill, Aberdeen AB 10 1FR, Scotland, United Kingdom

<sup>c</sup> Aristotle University of Thessaloniki, Faculty of Chemistry, Inorganic Chemistry Laboratory, P.O. Box 135, GR-541 24 Thessaloniki, Greece

Received 26 September 2006; accepted 1 December 2006

Available online 14 December 2006

## Abstract

Reaction of silver(I) bromide with equimolar amounts of the rigid diphos ligands 1,2-bis(diphenylphosphano)benzene (dppbz) and 4,5-bis(diphenylphosphano)-9,9-dimethyl-xanthene (xantphos) in acetone and acetonitrile led to the corresponding chelates  $[\text{Ag}(\mu_2\text{-Br})(\text{dppbz})]_2$  (**1**) and  $[\text{AgBr}(\text{xantphos})]$  (**2**). Treatment of **1** and **2** with pyridine-2-thione (py2SH) in ethanol gave the mixed-ligand complexes  $[\text{AgBr}(\text{dppbz})(\text{py2SH})]$  (**3**) and  $[\text{AgBr}(\text{xantphos})(\text{py2SH})]$  (**4**), respectively. Compounds **1**, **2** and **4** have been characterized by X-ray diffraction, establishing distorted tetrahedral or trigonal planar coordination geometries of the silver atoms.

© 2006 Elsevier Ltd. All rights reserved.

**Keywords:** Silver(I) complexes; Rigid diphosphanes; Pyridine-2-thione; Crystal structures

## 1. Introduction

Phosphanes are particularly appropriate for stabilizing low-valent metals ions, consequently there are numerous diphosphane containing silver(I) complexes [1]. In recent years, these complexes have attracted considerable attention because of their applications in several homogeneous catalytic processes [2]. Some of these complexes have also shown antitumour activity, as well as antifungal and antibacterial properties [3,4].

It is well known that variation in coordination number and nuclearity in complexes of closed-shell  $d^{10}$  metal ions can be induced by variation of the ligands bound to the

metal centre. Silver(I) can exhibit coordination numbers ranging from 2 to 4 with the preference for a given coordination number strongly depending on the nature of the ligands. In the specific case of oligomethylene-backboned diphosphanes of the type  $\text{Ph}_2\text{P}(\text{CH}_2)_n\text{PPh}_2$ , for instance, the coordination behaviour (chelating or bridging mode) primarily depends on the length of the methylene chain between the two P donors, leading to an extensive and varied family of compounds. Thus, for a given metal salt: diphosphane stoichiometry, the adducts formed may be monomeric chelated species, macrocyclic dimers in which the two metal centres are linked together by both bridging diphosphane and halide ligands, or even extended polymeric formations [5].

Besides the chain length of a bridging diphosphane, its bulkiness and flexibility have been recognized as additional significant factors in controlling product selectivity in the

\* Corresponding author.

E-mail addresses: [p.j.cox@rgu.ac.uk](mailto:p.j.cox@rgu.ac.uk) (P.J. Cox), [aslanidi@chem.auth.gr](mailto:aslanidi@chem.auth.gr) (P. Aslanidis).

formation of a multisilver complex. For instance, dinuclear (2:2) macrocycles are the most frequently encountered structural motifs for silver(I) salts with oxo-anions when long-chained flexible diphosphanes are used, whereby the rigid bis(diphenylphosphano)acetylene (dppa) selectively forms cationic disilver complexes with triply-bridging diphosphane units [6]. In this context, previous related work from our laboratory has also revealed the variety of structural motifs observed within a series of thione/phosphane ligated derivatives of Ag(I) halides or Ag(I) nitrate to be dependent on the choice of the bidentate phosphane ligand [7].

In the quest for new materials with specialized catalytic properties, investigations are directed at present towards the development of new fine-tuned ligands for catalytic systems with suitable activity and selectivity. For example, the use of sterically demanding diphosphanes as ligands in transition metal catalysed synthesis of chiral organic compounds is becoming a very intense area of study [8]. The P–M–P bite angle has been established to be an important parameter related to the properties of the catalysts. Concerning the later bite angle effect, considerable progress has been made since the development of new diphos ligands based on xanthene-type backbones [9]. In the course of our systematic structural studies on mixed-ligand coordination compounds of group 11 metals, we recently reported on the coordination capability of two sterically demanding and configurationally inflexible diphosphanes, namely 4,5-bis(diphenylphosphano)-9,9-dimethylxanthene (xantphos), the parent member of the extended xantphos ligand family, and 1,2-bis(diphenylphosphano)benzene (dppbz) towards copper(I) halides in the presence of heterocyclic thiones as co-ligands [10]. As these two diphosphanes, based on rigid aromatic backbones, produced different products to those of their extensively studied flexible counterparts, we decided to extend our studies to the analogous silver(I) halide complexes, starting in the present paper with the structural characterization of some derivatives of silver(I) bromide. In addition, these comparative studies could provide useful information regarding the dimerization frequently observed within this class of complexes.

## 2. Experimental

### 2.1. Materials and instruments

Commercially available silver bromide, 1,2-bis(diphenylphosphano)benzene (dppbz), 4,5-bis(diphenylphosphano)-9,9-dimethyl-xanthene (xantphos) were used as received while pyridine-2-thione (py2SH) was recrystallized from hot ethanol prior to use (Scheme 1). All the solvents were purified by their respective suitable methods and allowed to stand over molecular sieves. Infra-red spectra in the region of 4000–250  $\text{cm}^{-1}$  were obtained in KBr discs with a Perkin-Elmer FT-IR Spectrum 1 spectrophotometer, while a Perkin-Elmer-Hitachi 200 spectrophotometer was used to obtain the electronic absorption spectra.  $^1\text{H}$

NMR spectra were recorded on a Bruker AM 300 spectrometer at 25 °C with chemical shifts given in ppm referenced to internal TMS. Melting points were measured in open tubes with a STUART scientific instrument and are uncorrected. Molar conductivities, magnetic susceptibility measurements and elemental analyses for carbon, nitrogen and hydrogen were performed as described previously [11]. Thermogravimetric analyses were performed on a SETSYS-1200 machine with a DTG facility in dry nitrogen atmosphere. Sample sizes were in the range 8–10 mg and open Pt crucibles were used. The heating rate was 10°/min.

### 2.2. X-ray crystallographic study

Single crystals of **1** and **2** suitable for X-ray crystallographic study were grown by slow concentration over several days at ambient temperature of their acetone and acetonitrile mother liquid, respectively, whereas compound **4** was obtained from an ethanolic solution. X-ray diffraction data were collected on an Enraf-Nonius Kappa CCD area-detector diffractometer.

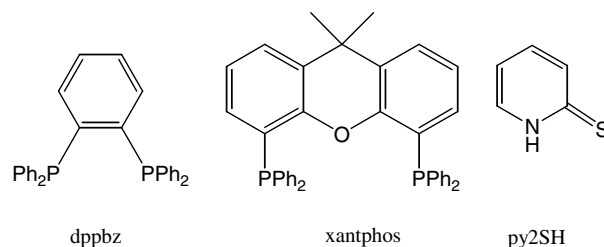
The programs DENZO [12] and COLLECT [13] were used in data collection and cell refinement. Details of crystal and structure refinement are shown in Table 1. The structures were solved using the program SIR 97 [14] and refined with the program SHELX-97 [15]. Molecular plots were obtained with the program ORTEP-3 [16].

### 2.3. Synthesis of compounds **1** and **2**

The homoleptic complexes were prepared according to the following general procedure. A suspension of silver bromide (47 mg, 0.25 mmol) and 0.25 mmol of the appropriate diphosphane (111.6 mg for dppbz or 144.7 mg for xantphos) in 60  $\text{cm}^3$  acetone or acetonitrile was refluxed for 2 h. The resulting mixture was filtered off and the clear solution was kept at room temperature. Slow evaporation of the solvent at room temperature gave the microcrystalline solid, which was filtered off and dried in vacuo.

### 2.4. $[\text{Ag}(\mu\text{-Br})(\text{dppbz})]_2$ (**1**)

Colourless crystals. Yield: 135 mg (85%), m.p. 298 °C; *Anal.* Calc. for  $\text{C}_{60}\text{H}_{48}\text{Ag}_2\text{Br}_2\text{P}_4$ : C, 56.81; H, 3.81. Found: C, 56.69; H, 3.91%. IR ( $\text{cm}^{-1}$ ): 3468m, 3051w, 1714s,



Scheme 1. The diphosphanes and the heterocyclic thione used as ligands, with their abbreviations.

Table 1  
Crystal data and structure refinement for **1**, **2** and **4**

	<b>1</b>	<b>2</b>	<b>4</b>
Chemical formula	C <sub>60</sub> H <sub>48</sub> Ag <sub>2</sub> Br <sub>2</sub> P <sub>4</sub> · C <sub>3</sub> H <sub>6</sub> O	C <sub>39</sub> H <sub>32</sub> AgBrOP <sub>2</sub>	C <sub>44</sub> H <sub>37</sub> AgBrNOP <sub>2</sub> S · C <sub>2</sub> H <sub>5</sub> OH
Formula weight	1326.50	766.37	923.59
Temperature (K)	120(2)	120(2)	120(2)
Wavelength (Å)	0.71073	0.71073	0.71073
Crystal system	triclinic	monoclinic	monoclinic
Space group	<i>P</i> $\bar{1}$	<i>P</i> 2 <sub>1</sub> / <i>m</i>	<i>P</i> 2 <sub>1</sub> / <i>n</i>
<i>Unit cell dimensions</i>			
<i>a</i> (Å)	11.4005(2)	8.7806(8)	10.17560(10)
<i>b</i> (Å)	11.9360(2)	18.1236(16)	21.4454(3)
<i>c</i> (Å)	21.4574(4)	12.2833(11)	19.2509(2)
$\alpha$ (°)	105.1170(10)	90	90
$\beta$ (°)	102.4180(10)	107.589(4)	98.5760(10)
$\gamma$ (°)	94.61	90	90
Volume (Å <sup>3</sup> )	2723.89(8)	1863.3(3)	4153.96(8)
<i>Z</i>	2	2	4
<i>D</i> <sub>calc</sub> (Mg/m <sup>3</sup> )	1.617	1.366	1.477
Absorption coefficient (mm <sup>−1</sup> )	2.346	1.726	1.613
<i>F</i> (000)	1328	772	1880
Crystal size (mm <sup>3</sup> )	0.18 × 0.08 × 0.06	0.36 × 0.22 × 0.06	0.42 × 0.28 × 0.18
$\theta$ Range for data collection (°)	3.04–27.53	3.38–27.49	3.30–27.4
Index ranges	−14 ≤ <i>h</i> ≤ 14, −15 ≤ <i>k</i> ≤ 15, −27 ≤ <i>l</i> ≤ 27	−11 ≤ <i>h</i> ≤ 11, −23 ≤ <i>k</i> ≤ 22, −15 ≤ <i>l</i> ≤ 15	−13 ≤ <i>h</i> ≤ 12, −27 ≤ <i>k</i> ≤ 27, −24 ≤ <i>l</i> ≤ 24
Reflections collected	51 314	16 003	57 932
Independent reflections [ <i>R</i> <sub>int</sub> ]	12 442 [0.0435]	4357 [0.0455]	9463 [0.0273]
Completeness to $\theta = 27.47^\circ$	99.1%	98.6%	99.6%
Maximum and minimum transmission	0.8721 and 0.6775	0.9035 and 0.5754	0.7600 and 0.5506
Refinement method	full-matrix least square on <i>F</i> <sup>2</sup>	full-matrix full-matrix least square on <i>F</i> <sup>2</sup>	full-matrix full-matrix least square on <i>F</i> <sup>2</sup>
Data /restraints/ parameters	12442/0/652	4357/21/225	9463/21/576
Goodness-of-fit on <i>F</i> <sup>2</sup> ( <i>S</i> )	1.011	1.039	1.046
Final <i>R</i> indices [ <i>I</i> > 2σ( <i>I</i> )]	<i>R</i> <sub>1</sub> = 0.0302, <i>wR</i> <sub>2</sub> = 0.0692	<i>R</i> <sub>1</sub> = 0.0652, <i>wR</i> <sub>2</sub> = 0.1860	<i>R</i> <sub>1</sub> = 0.0268, <i>wR</i> <sub>2</sub> = 0.0629
<i>R</i> indices (all data)	<i>R</i> <sub>1</sub> = 0.0408, <i>wR</i> <sub>2</sub> = 0.0739	<i>R</i> <sub>1</sub> = 0.0918, <i>wR</i> <sub>2</sub> = 0.1978	<i>R</i> <sub>1</sub> = 0.0316, <i>wR</i> <sub>2</sub> = 0.0654
Final weighting scheme	Calc <i>w</i> = 1/[σ <sup>2</sup> ( <i>F</i> <sub>o</sub> <sup>2</sup> ) + (0.0286 <i>P</i> ) <sup>2</sup> + 2.4902 <i>P</i> ], where <i>P</i> = ( <i>F</i> <sub>o</sub> <sup>2</sup> + 2 <i>F</i> <sub>c</sub> <sup>2</sup> )/3	Calc <i>w</i> = (1/[σ <sup>2</sup> ( <i>F</i> <sub>o</sub> <sup>2</sup> ) + (0.1153 <i>P</i> ) <sup>2</sup> + 3.4918 <i>P</i> ], where <i>P</i> = ( <i>F</i> <sub>o</sub> <sup>2</sup> + 2 <i>F</i> <sub>c</sub> <sup>2</sup> )/3)	Calc <i>w</i> = (1/[σ <sup>2</sup> ( <i>F</i> <sub>o</sub> <sup>2</sup> ) + (0.0263 <i>P</i> ) <sup>2</sup> + 3.3960 <i>P</i> ], where <i>P</i> = ( <i>F</i> <sub>o</sub> <sup>2</sup> + 2 <i>F</i> <sub>c</sub> <sup>2</sup> )/3)
Extinction coefficient	0.00135(11)		
Largest difference in peak and hole (e Å <sup>−3</sup> )	0.515 and −0.677	2.486 and −1.136	0.442 and −1.365

1479s, 1435vs, 1216s, 1098s, 1026s, 761s, 745vs, 729s, 691vs, 506vs, 495s, 477s; UV–Vis ( $\lambda_{\text{max}}$ , log  $\epsilon$ ): (CHCl<sub>3</sub>); 249 (3.77), 269 (3.74), 297 (3.38). <sup>1</sup>H NMR (CDCl<sub>3</sub>,  $\delta$  ppm): 7.38–7.01 (m, 24H, 4C<sub>6</sub>H<sub>5</sub>+C<sub>6</sub>H<sub>4</sub>).

## 2.5. [AgBr(*xantphos*)] · CH<sub>3</sub>CN (**2**)

Colourless crystals. Yield: 186 mg (92%), m.p. 338 °C; *Anal.* Calc. for C<sub>41</sub>H<sub>35</sub>AgBrNOP<sub>2</sub>: C, 60.99; H, 4.37; N, 1.73. Found: C, 60.62; H, 4.23; N, 1.57%. IR (cm<sup>−1</sup>): 3437m, 3049w, 2975w, 1480m, 1435s, 1405vs, 1238s, 1097m, 1027m, 789s, 746vs, 695vs, 509vs, 457s; UV–Vis

( $\lambda_{\text{max}}$ , log  $\epsilon$ ): (CHCl<sub>3</sub>); 253 (3.76). <sup>1</sup>H NMR (CDCl<sub>3</sub>,  $\delta$  ppm): 7.58 (d, 1H, H<sup>3</sup><sub>xantphos</sub>), 7.30 (m, 8H, PC<sub>6</sub>H<sub>5</sub>), 7.20 (m, 12H, PC<sub>6</sub>H<sub>5</sub>), 7.06 (dd, 1H, H<sup>3</sup><sub>xantphos</sub>), 6.58 (d, 1H, H<sup>1</sup><sub>xantphos</sub>), 1.67 (s, 6H, H<sub>3</sub>C<sub>xantphos</sub>).

## 2.6. Synthesis of compounds **3** and **4**

The heteroleptic complexes were prepared according to the following general procedure. A suspension of silver bromide (47 mg, 0.25 mmol) and 0.25 mmol of the appropriate diphosphane (111.6 mg for dppbz or 144.7 mg for *xantphos*) in 40 cm<sup>3</sup> ethanol was refluxed for 2 h until a

white precipitation formed. A solution of pyridine-2-thione (28 mg, 0.25 mmol) in ethanol was treated with a small quantity of pyridine and was then added dropwise to the hot suspension and the reaction mixture was refluxed for an additional 2 h. The resulting solution was filtered off and the clear yellow solution was kept at room temperature. Slow evaporation of the solvent at room temperature gave the microcrystalline solid, which was filtered off and dried in vacuo.

### 2.7. $[AgBr(dppbz)(py2SH)]$ (**3**)

Pale yellow crystals. Yield: 158 mg (85%), m.p. 253 °C; *Anal.* Calc. for  $C_{35}H_{29}AgBrNP_2S$ : C, 56.40; H, 3.92; N, 1.88. Found: C, 55.90; H, 4.20; N, 1.68%. IR ( $cm^{-1}$ ): 3437m, 3155w, 3047w, 1614s, 1596s, 1556vs, 1479s, 1436vs, 1216m, 1135vs, 1095s, 1025m, 986m, 751vs, 730s, 694vs, 513vs, 488s, 447m; UV–Vis ( $\lambda_{max}$ , log  $\epsilon$ ): ( $CHCl_3$ ); 245 (4.31), 274 (4.15), 298 (4.06).  $^1H$  NMR ( $CDCl_3$ ,  $\delta$  ppm): 7.46 (dd, 1H,  $H_{py2SH}^6$ ), 7.38–7.06 (m, 24H,  $4C_6H_5 + C_6H_4$ ) 7.30 (overlapping t, 1H,  $H_{py2SH}^4$ ), 6.68 (t, 1H,  $H_{py2SH}^5$ ).

### 2.8. $[AgBr(xantphos)(py2SH)] \cdot C_2H_5OH$ (**4**)

Yellow crystals. Yield: 62 mg (27%), m.p. 279 °C; *Anal.* Calc. for  $C_{46}H_{43}AgBrNO_2P_2S$ : C, 59.82; H, 4.69; N, 1.51. Found: C, 59.85; H, 4.64; N, 1.41%. IR ( $cm^{-1}$ ): 3453m, 3148w, 3051w, 2963m, 1617s, 1570vs, 1480m, 1434vs, 1404vs, 1367m, 1230vs, 1134vs, 1094m, 1028m, 991m, 791m, 749vs, 729s, 694vs, 511vs, 484s, 462s; UV–Vis ( $\lambda_{max}$ , log  $\epsilon$ ): ( $CHCl_3$ ); 248 (4.43), 281 (4.43), 373 (3.71).  $^1H$  NMR ( $CDCl_3$ ,  $\delta$  ppm): 7.52 (d, 1H,  $H_{xantphos}^3$ ), 7.49 (dd, 1H,  $H_{py2SH}^6$ ), 7.40 (m, 8H,  $PC_6H_5$ ), 7.32 (overlapping t, 1H,  $H_{py2SH}^4$ ), 7.24 (m, 12H,  $PC_6H_5$ ), 7.04 (dd, 1H,  $H_{xantphos}^2$ ), 6.72 (d, 1H,  $H_{xantphos}^1$ ), 6.60 (t, 1H,  $H_{py2SH}^5$ ), 1.63 (s, 6H,  $H_3C_{xantphos}$ ).

## 3. Results and discussion

### 3.1. Preparative considerations

The reaction between equimolar quantities of silver(I) bromide and 1,2-bis(diphenylphosphano)benzene (dppbz) or 4,5-bis(diphenyl-phosphano)-9,9-dimethyl-xanthene (xantphos) in dry acetone or acetonitrile afforded microcrystalline solids which, on elemental analysis, were found to be of the composition  $[AgBr(diphos)]$  (compounds **1** and **2**, respectively). It should be pointed out that both diphosphanes showed a strong preference for chelation at a single metal centre in their reactions with copper(I) halides [10], despite of the marked difference in their natural bite angles. This coordination behaviour undoubtedly demonstrates their strong chelating power but should be also ascribed, to a significant degree, to the extraordinary versatility of a  $d^{10}$  metal ion and therefore chelation was expected to be preferred over bridging also in the case of silver(I). On

the other hand, there is a well known tendency for copper(I) and to a lesser extent for silver(I) to achieve the common four-coordination forming dinuclear species involving halide ligands in a  $\mu_2-X$  bridging mode. Thus, according to our previous experience, particularly with dppbz, compounds **1** and **2** were expected to be halide-bridged dimers of type  $[Ag(\mu_2-Br)(diphos)]_2$ . X-ray crystal structure determinations showed, however, that this is the case only for the dppbz derivative, whereas compound **2** is a three-coordinated monomer.

Following the one-pot two-step synthetic procedure that has proven to produce mixed-ligand copper(I) and silver(I) complexes virtually for any heterocyclic thione, we next attempted the preparation of heteroleptic complexes of the type  $[AgBr(diphos)(thione)]$ . In particular, we prepared suspensions of compounds **1** and **2** in dry acetonitrile and treated these with an equimolar quantity of a methanolic solution of the appropriate thione. Heating of the mixture at reflux for several hours did not caused, as expected, the disappearance of the white precipitate, indicating the presence of unreacted starting material. Indeed, the white amorphous solid isolated by filtration could be identified as compounds **1** and **2**, respectively. On the other hand, the composition of the microcrystalline solid that was obtained on evaporation of the yellow solution at ambient temperature changed over time as a function of the evaporation state, indicating the presence of a product mixture. Surprisingly, only in the case of py2SH did the reaction proceed towards the expected products, employing an ethanol/pyridine mixture as solvent, which may seem quite unusual and was initially used to possibly favour deprotonation of the thione, thus to increase its coordination capability. It should be, however, anticipated that both  $[AgBr(dppbz)(py2SH)]$  (**3**) and  $[AgBr(xantphos)(py2SH)]$  (**4**) still contain the thione unit in its neutral (protonated) form.

All the prepared complexes are microcrystalline solids, slightly soluble in acetonitrile and only marginally soluble in chloroform and acetone. They are stable to air and moisture and can be manipulated in air without appreciable decomposition. Their solutions in acetonitrile exhibit no conductivity. Room temperature magnetic measurements confirm the expected diamagnetic nature of the compounds.

### 3.2. Spectroscopic characterization

The solid state FT-IR spectra of the four compounds, recorded in the range 4000–250  $cm^{-1}$ , show all the expected strong phosphane bands, which remain practically unshifted upon coordination. Moreover the spectra of the mixed-ligand complexes **3** and **4** contain the four characteristic “thioamide bands” required by the presence of the heterocyclic thioamide, with shifts suggestive of its coordination mode. “Thioamide(IV)”, for instance, which appears at 742  $cm^{-1}$  in the spectrum of the “free” pyridine-2-thione and mainly involves contribution from the  $\nu(C=S)$  vibration, undergoes a significant downward shift

(by more than  $30\text{ cm}^{-1}$ ) upon coordination, indicating M–S bond formation. The thione form of the coordinated heterocyclic thioamide is further established by the presence of the NH stretching vibration at  $3159$  and  $3149\text{ cm}^{-1}$  for **3** and **4**, respectively, in combination with the lack of an S–H stretching band around  $2560\text{ cm}^{-1}$ .

The room temperature  $^1\text{H}$  NMR spectra of the complexes, recorded in deuterated chloroform, are dominated by the presence of complex multiplets in the  $7.20$ – $7.40$  ppm region due to phenyl/phenylene resonances, as well as, in the case of compounds **3** and **4**, signals attributable to the aromatic protons of the pyridine-2-thione unit. Upon coordination, the multiplets assigned to the  $\text{PPh}_2$  groups of the phosphane ligands undergo splitting due to a small upfield shift of the *ortho*-positioned protons, whereas the signals of the corresponding backbone protons remain practically unshifted.

The electronic absorption spectra of compounds **1** and **2** in chloroform solutions appear to be mainly of intraligand character, consisting of three or one intense sharp band respectively (see Section 2). These bands can be attributed to intraligand  $\pi^* \leftarrow \pi$  transitions on the phenyl group of the phosphane ligands, since the uncoordinated 1,2-bis(diphenylphosphano)benzene and 4,5-bis(diphenylphosphano)-9,9-dimethyl-xanthene reveal three or one strong absorptions respectively at  $245$ ,  $273$  and  $299\text{ nm}$  or  $264\text{ nm}$ , all of them undergoing small shifts upon coordination to  $\text{Ag(I)}$ . The spectra of complexes **3** and **4** show an additional lower energy band that lies in the region where the free thione absorbs, expressing a small red shift as a consequence of the coordination to  $\text{Ag(I)}$  and should be, therefore, considered as a thione-originating intraligand transition which possesses some MLCT character [17].

### 3.3. Thermal decomposition

The thermal behaviour of the new compounds was investigated using simultaneous differential thermoanalysis (DTA) and thermogravimetry (TG) in a nitrogen atmosphere. TG and DTA data curves for compounds  $[\text{AgBr}(\text{xantphos})]$  (**2**) and  $[\text{AgBr}(\text{xantphos})(\text{py}2\text{SH})]$  (**4**) are given in Fig. 1.

Complexes **1** and **2** decompose in one single stage that starts at  $330$  or  $390\text{ }^\circ\text{C}$ , respectively and extends over a temperature range of  $100\text{ }^\circ\text{C}$ . The observed mass loss notified by the TG curve fits in each case perfectly as the loss of the diphosphane, whereby the corresponding DTA curve shows a strong endothermic effect. Complexes **3** and **4** show the typical decomposition pattern observed for the analogous copper(I) halide compounds [10a,10c], generally consisting of two main stages, the low temperature initial stage, observed in the TG curve in the  $240$ – $280\text{ }^\circ\text{C}$  range, being connected with two endothermic events in the DTA curve and involving overall weight loss indicative of gradual thermal breakdown of the pyridine-2-thione ligand. A very strong endothermic event appears at about  $380\text{ }^\circ\text{C}$ , which does not affect the consistency of the compounds,

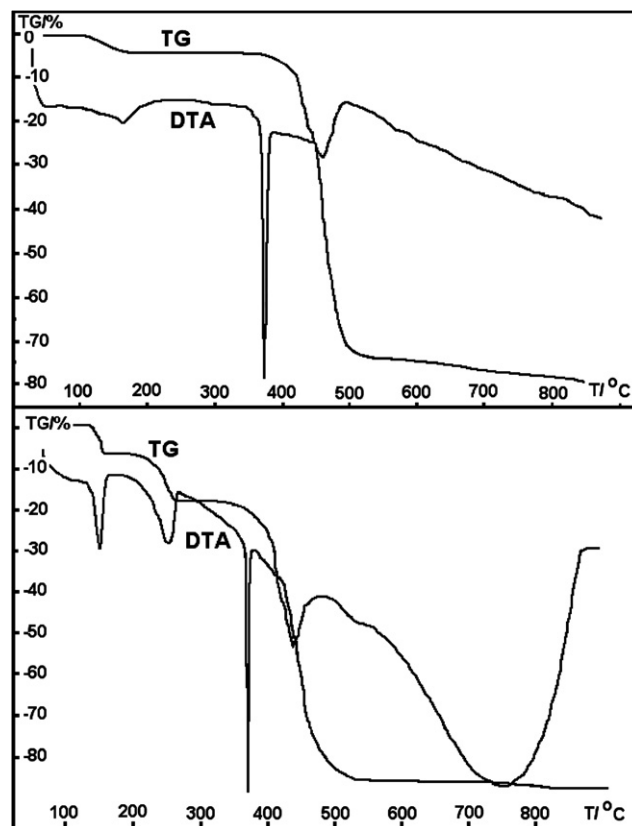


Fig. 1. TG and DTA curves for  $[\text{AgBr}(\text{xantphos})]$  (**2**) and  $[\text{AgBr}(\text{xantphos})(\text{py}2\text{SH})]$  (**4**).

in any form. In the case of compounds **2** and **4** solvent retention occurs at the temperature  $170\text{ }^\circ\text{C}$ , indicated by a weak endothermic effect. For all the compounds further heating causes gradual sublimation of the residual  $\text{AgBr}$  which is almost completely removed at  $980\text{ }^\circ\text{C}$ .

### 3.4. Crystal structures

The X-ray crystal structures of  $[\text{Ag}(\mu_2\text{-Br})(\text{dppbz})_2]$  (**1**),  $[\text{AgBr}(\text{xantphos})]$  (**2**) and  $[\text{AgBr}(\text{xantphos})(\text{py}2\text{SH})]$  (**4**) (details of crystal and structure refinement are shown in Table 1) corroborate the spectroscopic results discussed above. Note that many heavy transition metal complexes with xantphos or dppbz have been described in the literature, but no  $\text{Ag}^{\text{I}}$  complexes are known to be structurally characterized by X-ray crystallography.

Colorless crystals of **1** suitable for X-ray crystallography were grown from its acetone mother liquid by slow evaporation at ambient temperature. The complex crystallizes in the triclinic space group  $P\bar{1}$  with two formula units in the unit cell. The asymmetric unit consists of two half-molecules as well as one acetone molecule, which will not be further discussed as there is no evidence of any specific interaction involving this latter solvent molecule. Respective bond lengths and angles within the two half-molecules are slightly different, thus two different centrosymmetric molecules (A and B) result by suitable symmetry transformations.



Fig. 2 depicts a perspective of one of these molecules showing the atom numbering. Bond lengths and angles around the Ag<sup>I</sup> centre are listed in Table 2.

The crystal structure contains a center of symmetry and features a dinuclear unit in which the two silver(I) centers are joined by two bromine bridges to form a “diamond-shaped” Ag<sub>2</sub>Br<sub>2</sub> core with Ag–Br–Ag and Br–Ag–Br bond angles that clearly deviate from the ideal values for symmetric dimers (70.5° and 109.5°) but are very close to the ideal geometry for Y<sub>2</sub>MX<sub>2</sub>MY<sub>2</sub> dimers according to theoretically proposed criteria [18]. The Ag<sup>+</sup>–Ag separation of 3.4985(3) Å is slightly longer than the sum of the van der Waals radii [19], thus excluding any possible metal–metal attractive interaction. It should be noted that, unlike the remarkable non-planarity within the Cu<sub>2</sub>Br<sub>2</sub> moiety of the recently reported [Cu(μ<sub>2</sub>-Br)(dppbz)]<sub>2</sub> [10b], complex **1** displays a strictly planar central core commonly adopted by halide-bridged dimeric complexes. Another noticeable difference between the two structures arises from the P–M–P intraligand angles, the acute P(1)–Ag(1)–P(2) bite-angle of 79.596(19)° in the present structure being clearly smaller than the corresponding P–Cu–P angles found in the above mentioned copper counterpart, which certainly can be ascribed to the different M–P bond lengths.

As expected, the carbon atoms of the phenylene backbone and the two adjacent phosphorus atoms are nearly coplanar, but the AgPCCP five-membered ring adopts an envelope conformation with the metal atom displaced out of the plane containing the four diphos ligand atoms by 1.2773(15) Å. The two phenyl rings on each phosphorus atom are nearly perpendicular to each other. However,

Table 2

Selected bond lengths (Å) and angles (°) for **1**

Ag(1)–P(1)	2.5142(6)	P(1)–C(7)	1.822(2)
Ag(1)–P(2)	2.5260(6)	P(1)–C(13)	1.819(2)
Ag(1)–Br(1)	2.6343(3)	P(2)–C(2)	1.839(2)
Ag(1)–Br(1)#	2.7521(3)	P(2)–C(19)	1.832(2)
P(1)–C(1)	1.830(2)	P(2)–C(25)	1.826(2)
P(1)–Ag(1)–P(2)	79.596(19)	Ag(1)–Br(1)–Ag(1)#	80.978(8)
P(1)–Ag(1)–Br(1)	121.404(16)	Ag(1)–P(1)–C(1)	101.27(7)
P(2)–Ag(1)–Br(1)	132.078(16)	Ag(1)–P(1)–C(7)	114.08(7)
P(1)–Ag(1)–Br(1)#	113.198(15)	Ag(1)–P(2)–C(2)	100.37(7)
P(2)–Ag(1)–Br(1)#	111.605(15)	Ag(1)–P(2)–C(19)	115.64(8)
Ag(1)–P(2)–C(19)	115.64(8)	P(1)–C(1)–C(2)	119.61(16)
Br(1)–Ag(1)–Br(1)#	99.022(8)	P(2)–C(2)–C(1)	119.30(16)

Symmetry transformations used to generate equivalent atoms: #  $-x + 1, -y + 1, -z + 1$ .

the C(7)–C(12) and C(19)–C(24) phenyl rings have their planes in an almost parallel arrangement as a consequence of a 3.6400(14) Å  $\pi$ -stacking interaction between them. Within the Ag<sub>2</sub>Br<sub>2</sub> backbone there are two different Ag–Br bond distances that are somewhat shorter than those found in other tetracoordinate silver(I) phosphane complexes, e.g. in [Ag(μ<sub>2</sub>-Br)(pymtH)]<sub>2</sub> [20]. Finally, the two Ag–P distances of 2.5142(6) Å and 2.5260(6) Å are within the limits of the value range expected for tetrahedrally coordinated Ag<sup>I</sup>.

Structure refinement for compound **2** was performed in both  $P2_1$  and  $P2_1/m$  monoclinic space groups and the higher symmetry space group  $P2_1/m$  was adopted. However, disorder involving the Br atom position (split over two sites), a poorly defined solvent molecule (occupying

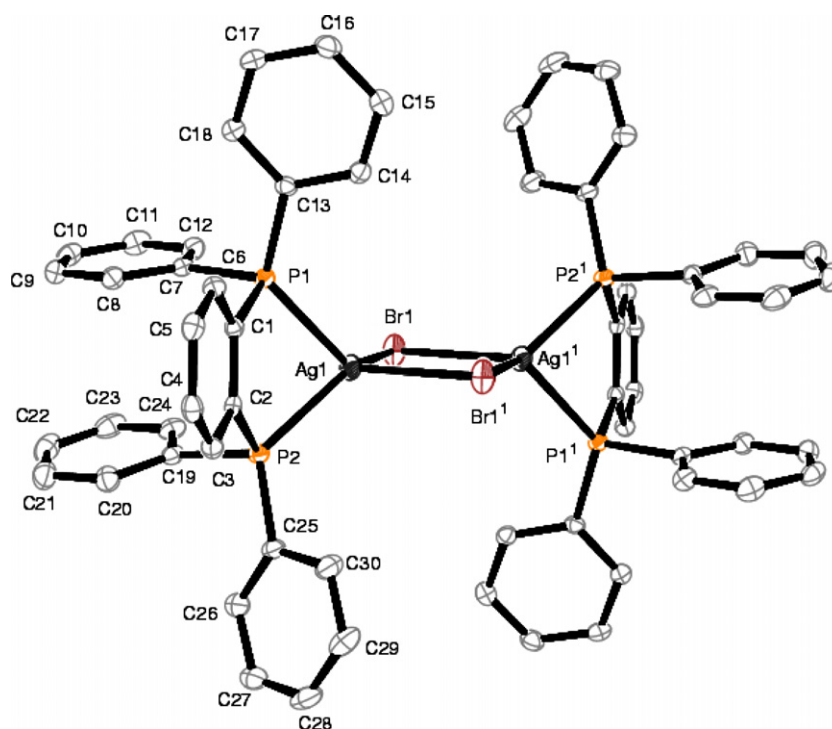


Fig. 2. Molecular structure of complex **1** with atom labels. Displacement ellipsoids are shown at the 50% probability level.

17% of the crystal volume, 18 electrons removed by PLATON [21] and some residual electron density spread along the 2-fold axis led to a structure less well defined than **1** or **4**. Fig. 3 depicts a perspective of the molecule showing the atom labelling scheme. Selected bond lengths and angles are listed in Table 3.

Contrary to the above discussed structure of the silver/dppbz complex, the xantphos derivative is a monomer, the inability for dimerization caused most probably by the marked steric demands of the bulky diphos ligand, expressed by its wide P–Ag–P bite angle versus the corresponding acute bite angle in the structure of **1**. Thus, the silver(I) metal exhibits a distorted trigonal coordination environment surrounded by two phosphorus atoms of the chelating xantphos as well as one bromine atom, with quite small angular deviations from the ideal trigonal value of  $120^\circ$  being mainly directed by the diphosphine bite angle. The crystal structure possess a symmetry plane defined by the C(1), C(8), C(9), O(1), Ag(1) and Br(1a) atoms, which require the  $P_2AgBr$  central core to be strictly planar. The smallest angle within this core corresponds to the P(1)–Ag(1)–P(1)# angle, whose value of  $109.38(7)^\circ$  is very close to the ligands calculated “natural” bite angle of  $111^\circ$  [21], indicating the extraordinary versatility of the closed shell central metal ion. Nevertheless, some adjustment on the part of the diphos ligand seems to be unavoidable in order to act as a chelate, which is expressed by the folding of the xanthene unit along its symmetry axis. In fact, the dihedral angle between the planes of the two benzenoid rings form a dihedral angle of  $150.3(2)^\circ$  whereas a value of  $156.58^\circ$  was found for the “free” xanthene molecule [21].

Compound **4** crystallizes in the monoclinic space group  $P2_1/n$  with four formula units in the unit cell. Fig. 4 depicts a perspective of the molecule showing the atom numbering.

Table 3

Selected bond lengths (Å) and angles ( $^\circ$ ) for **2**

Ag(1)–P(1)	2.4478(14)	P(1)–C(6)	1.829(6)
		P(1)–C(10)	1.831(6)
Ag(1)–Br(1a)	2.658(7)		
P(1)–Ag(1)–P(1)#	109.38(7)	C(16)–P(1)–C(6)	104.3(3)
P(1)–Ag(1)–Br(1a)	125.31(4)	C(6)–P(1)–C(10)	103.1(2)
		P(1)–C(6)–C(5)	123.2(4)
Ag(1)–P(1)–C(16)	111.62(19)	P(1)–C(6)–C(7)	118.8(4)

Symmetry transformation used to generate equivalent atoms:  $x, -y + 0.5, z$ .

Bond lengths and angles around the  $Ag^I$  are listed in Table 4. Two P donors, one S donor of the heterocyclic thione and the bromine atom form a fairly regular tetrahedron, where the angles around the silver atom vary from  $103.300(18)^\circ$  for S(1)–Ag(1)–Br(1) to  $117.13(3)^\circ$  for P(2)–Ag(1)–S(1). Interestingly, upon chelation the xantphos ligand exactly retains its “natural” bite angle [21].

The geometrical characteristics of the structure under investigation generally refer to those of other silver(I) complexes tetrahedrally coordinated by phosphine and thione ligands. Thus, the two Ag–P distances vary little [Ag(1)–P(1) =  $2.4843(5)$  and Ag(1)–P(2) =  $2.4994(5)$  Å] and lie at the upper limit of values found for a number of complexes containing tetracoordinated silver atoms bonded to two phosphorus atoms [7b]. The Ag–S bond distance of  $2.5395(5)$  Å, coincident with the sum of the corresponding atomic radii, is typical for this bonding arrangement. Finally, hydrogen bonds of type  $N-H \cdots Br$  and  $O-H \cdots Br$  (from the ethanol molecule) are observed, as well as a weak intramolecular  $\pi$ – $\pi$  stacking interaction between the C(33) and C(38) phenyl ring of the xantphos unit and the heterocyclic thione ring.

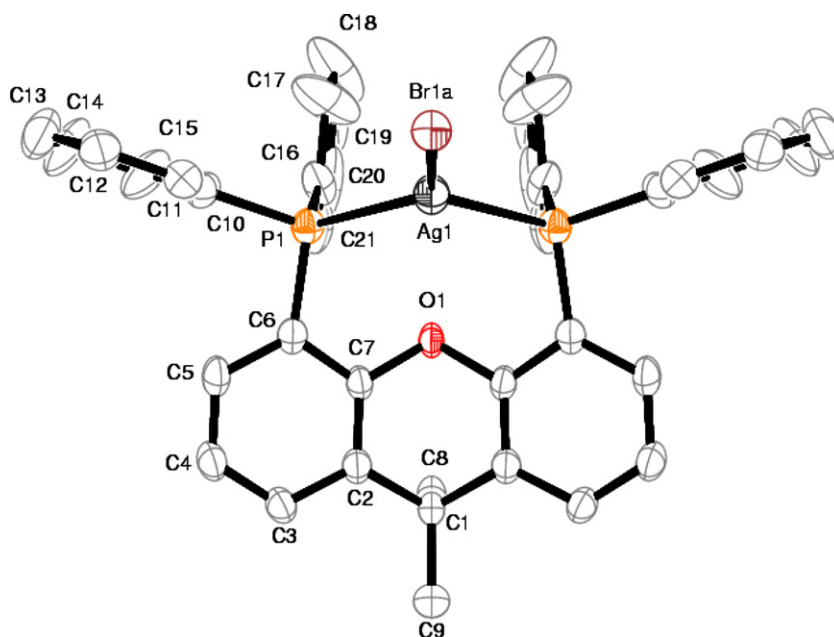


Fig. 3. Molecular structure of complex **2** with disorder removed. Displacement ellipsoids are shown at the 50% probability level.

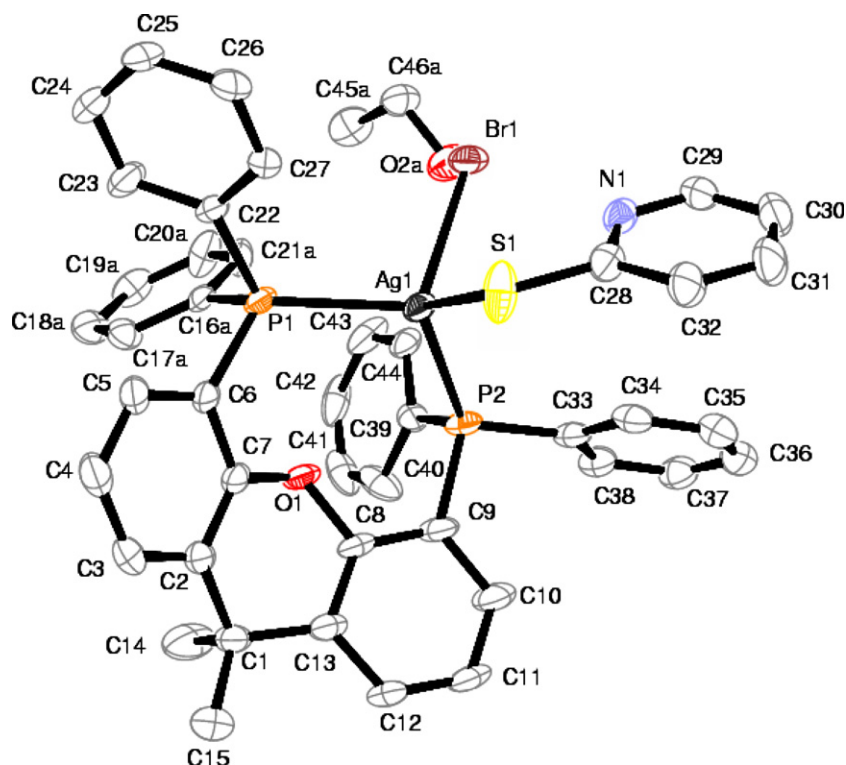


Fig. 4. Molecular structure of complex **4** with atom labels. Displacement ellipsoids are shown at the 50% probability level.

Table 4  
Selected bond lengths (Å) and angles (°) for **4**

<i>Bond length</i>			
Ag(1)–P(1)	2.4843(5)	Ag(1)–Br(1)	2.8587(3)
Ag(1)–P(2)	2.4994(5)	S(1)–C(28)	1.703(2)
Ag(1)–S(1)	2.5395(5)		
<i>Bond angle</i>			
P(1)–Ag(1)–P(2)	111.507(17)	P(2)–Ag(1)–Br(1)	104.460(13)
P(1)–Ag(1)–S(1)	112.602(18)	S(1)–Ag(1)–Br(1)	103.300(18)
P(2)–Ag(1)–S(1)	117.13(3)	C(28)–S(1)–Ag(1)	106.16(7)
P(1)–Ag(1)–Br(1)	106.564(13)		
<i>Hydrogen bridges</i>			
N(1)–H(1)	0.8800	N(1)···Br(1)	3.2945(17)
NH(1)–Br(1)	2.4200	Br(1)···H(1)–N(1)	172.0
O(2A)–H(2A)	0.8400	O(2A)···Br(1)	3.577(6)
OH(2A)–Br(1)	2.7400	Br(1)···H(2A)–O(2A)	173

#### 4. Conclusion

The aim of this work was the study of the coordination capability of the diphos ligands 1,2-bis(diphenylphosphano)benzene (dppbz) and 4,5-bis(diphenylphosphano)-9,9-dimethylxanthene (xantphos) toward silver(I) bromide. We have found that, despite the quite different geometrical characteristics of the two diphosphanes, xantphos providing a much larger bite angle than the acute bite angle of dppbz, chelation was observed as the only coordination mode for both diphos ligands. Compounds of the same composition [AgX(diphos)], but of different geometry and nuclearity were formed, namely a halide bridged dimer

with tetrahedrally coordinated Ag<sup>I</sup> centers for dppbz and monomeric trigonal in the case of xantphos. Both complexes proved to be good precursors for the preparation of mixed ligand monomeric complexes which contain, besides the chelating diphos unit, a heterocyclic thioamide bonded to the metal via the thione-S atom. According to the overall geometries of the structures presented, the xantphos ligand applied can be considered as best tailored for chelation of silver(I) centres.

#### 5. Supplementary material

CCDC 612754, 612755 and 612756 contain the supplementary crystallographic data for **1**, **2** and **4**. These data can be obtained free of charge via <http://www.ccdc.cam.ac.uk/conts/retrieving.html>, or from the Cambridge Crystallographic Data Centre, 12 Union Road, Cambridge CB2 1EZ, UK; fax: (+44) 1223-336-033; or e-mail: [deposit@ccdc.cam.ac.uk](mailto:deposit@ccdc.cam.ac.uk).

#### Acknowledgements

We thank the EPSRC X-ray crystallography service at the University of Southampton for collecting the X-ray data.

#### References

- [1] Effendy, C. di Nicola, M. Fianchini, C. Pettinari, B.W. Skelton, N. Somers, A.H. White, *Inorg. Chim. Acta* 357 (2004) 1523, and references therein.



- [2] M. Sawamura, H. Hamashima, Y. Ito, *J. Org. Chem.* 55 (1990) 5935.
- [3] S.J. Berners-Price, R.K. Johnson, A.J. Giovenella, L.F. Faucette, C.K. Mirabelli, P.J. Sadler, *J. Inorg. Biochem.* 33 (1988) 285.
- [4] C.S.W. Harker, E.R.T. Tiekink, *J. Coord. Chem.* 21 (1990) 287.
- [5] Effendy, C. di Nicola, M. Fianchini, C. Pettinari, B.W. Skelton, N. Somers, A.H. White, *Inorg. Chim. Acta* 358 (2005) 763.
- [6] (a) S.L. James, E. Lozano, M. Nieuwenhuyzen, *Chem. Commun.* (2000) 617;  
(b) E. Lozano, M. Nieuwenhuyzen, S.L. James, *Chem. Eur. J.* (2001) 2644.
- [7] (a) P. Aslanidis, P.J. Cox, S. Divanidis, P. Karagiannidis, *Inorg. Chim. Acta* 357 (2004) 2677;  
(b) P. Aslanidis, S. Divanidis, P.J. Cox, P. Karagiannidis, *Polyhedron* 24 (2005) 853.
- [8] R. Noyori, *Asymmetric Catalysis in Organic Synthesis*, Wiley, New York, 1994.
- [9] (a) M. Kranenburg, Y.E.M. van der Burgt, P.C.J. Kamer, P.W.N.M. Leeuwen, *Organometallics* 14 (1995) 3081;  
(b) L.A. van der Veen, M.D.K. Boele, F.R. Bregman, P.C.J. Kamer, P.W.N.M. van Leeuwen, K. Goubitz, J. Fraanje, H. Schenk, C. Bo, *J. Am. Chem. Soc.* 120 (1998) 11616;  
(c) L.A. van der Veen, P.H. Keeven, G.C. Schoemaker, J.N.H. Reek, P.C.J. Kamer, P.W.N.M. van Leeuwen, M. Lutz, A.L. Spek, *Organometallics* 19 (2000) 872.
- [10] (a) A. Kaltzoglou, P.J. Cox, P. Aslanidis, *Inorg. Chim. Acta* 358 (2005) 3048;  
(b) P. Aslanidis, P.J. Cox, A. Kaltzoglou, A.C. Tsipis, *Eur. J. Inorg. Chem.* (2006) 334;  
(c) P.J. Cox, A. Kaltzoglou, P. Aslanidis, *Inorg. Chim. Acta* 359 (2006) 3183.
- [11] P. Karagiannidis, P. Aslanidis, S. Papastefanou, D. Mentzafos, A. Hountas, A. Terzis, *Polyhedron* 9 (1990) 981.
- [12] Z. Otwinowski, W. Minor, in: C.W. Carter Jr., R.M. Sweet (Eds.), *Methods in Enzymology, Macromolecular Crystallography*, vol. 276, Academic Press, 1997, Part A, 307.
- [13] R. Hooft, *COLLECT Data Collection Software*, Nonius B.V., 1998.
- [14] A. Altomare, M.C. Burla, M. Camalli, G.L. Cascarano, C. Giacovazzo, A. Guagliardi, A.G.G. Moliterni, G. Polidori, R. Spagna, *J. Appl. Cryst.* 27 (1994) 434.
- [15] G.M. Sheldrick, *SHELXL-97. Program for Crystal Structure Analysis* (Release 97-2), University of Goettingen, Germany, 1997.
- [16] L.J. Farrugia, *J. Appl. Crystallogr.* 30 (1977) 565.
- [17] (a) A.A. Del Paggio, D.R. McMillin, *Inorg. Chem.* 22 (1983) 691;  
(b) C. Kutal, *Coord. Chem. Rev.* 99 (1990) 213.
- [18] R.H. Summerville, R. Hoffmann, *J. Am. Chem. Soc.* 98 (1976) 7240.
- [19] A. Bondi, *J. Phys. Chem.* 68 (1964) 441.
- [20] G.A. Bowmaker, Effendy, J.V. Hanna, P.C. Healy, B.W. Skelton, A.H. White, *J. Chem. Soc., Dalton Trans.* (1993) 1387.
- [21] S. Hildebrand, J. Bruckmann, C. Krüger, M.W. Haenel, *Tetrahedron Lett.* 36 (1995) 75.